NASA/TM—2011-217015

Material Characterization and Geometric Segmentation of a Composite Structure Using Microfocus X-Ray Computed Tomography Image-Based Finite Element Modeling

Ali Abdul-Aziz and D.J. Roth
Glenn Research Center, Cleveland, Ohio

R. Cotton
Simpleware Ltd., Exeter, United Kingdom

George F. Studor and Eric Christiansen
Johnson Space Center, Houston, Texas

P.C. Young
University of Exeter, Exeter, United Kingdom

July 2011

NASA STI Program . . . in Profile

Since its founding, NASA has been dedicated to the advancement of aeronautics and space science. The NASA Scientific and Technical Information (STI) program plays a key part in helping NASA maintain this important role.

The NASA STI Program operates under the auspices of the Agency Chief Information Officer. It collects, organizes, provides for archiving, and disseminates NASA's STI. The NASA STI program provides access to the NASA Aeronautics and Space Database and its public interface, the NASA Technical Reports Server, thus providing one of the largest collections of aeronautical and space science STI in the world. Results are published in both non-NASA channels and by NASA in the NASA STI Report Series, which includes the following report types:

- TECHNICAL PUBLICATION. Reports of completed research or a major significant phase of research that present the results of NASA programs and include extensive data or theoretical analysis. Includes compilations of significant scientific and technical data and information deemed to be of continuing reference value. NASA counterpart of peer-reviewed formal professional papers but has less stringent limitations on manuscript length and extent of graphic presentations.

- TECHNICAL MEMORANDUM. Scientific and technical findings that are preliminary or of specialized interest, e.g., quick release reports, working papers, and bibliographies that contain minimal annotation. Does not contain extensive analysis.

- CONTRACTOR REPORT. Scientific and technical findings by NASA-sponsored contractors and grantees.

- CONFERENCE PUBLICATION. Collected papers from scientific and technical conferences, symposia, seminars, or other meetings sponsored or cosponsored by NASA.

- SPECIAL PUBLICATION. Scientific, technical, or historical information from NASA programs, projects, and missions, often concerned with subjects having substantial public interest.

- TECHNICAL TRANSLATION. English-language translations of foreign scientific and technical material pertinent to NASA's mission.

Specialized services also include creating custom thesauri, building customized databases, organizing and publishing research results.

For more information about the NASA STI program, see the following:

- Access the NASA STI program home page at *http://www.sti.nasa.gov*

- E-mail your question via the Internet to *help@sti.nasa.gov*

- Fax your question to the NASA STI Help Desk at 443–757–5803

- Telephone the NASA STI Help Desk at 443–757–5802

- Write to:
  NASA Center for AeroSpace Information (CASI)
  7115 Standard Drive
  Hanover, MD 21076–1320

NASA/TM—2011-217015

Material Characterization and Geometric Segmentation of a Composite Structure Using Microfocus X-Ray Computed Tomography Image-Based Finite Element Modeling

Ali Abdul-Aziz and D.J. Roth
Glenn Research Center, Cleveland, Ohio

R. Cotton
Simpleware Ltd., Exeter, United Kingdom

George F. Studor and Eric Christiansen
Johnson Space Center, Houston, Texas

P.C. Young
University of Exeter, Exeter, United Kingdom

National Aeronautics and
Space Administration

Glenn Research Center
Cleveland, Ohio 44135

July 2011

This report contains preliminary findings, subject to revision as analysis proceeds.

Level of Review: This material has been technically reviewed by technical management.

Available from

NASA Center for Aerospace Information
7115 Standard Drive
Hanover, MD 21076–1320

National Technical Information Service
5301 Shawnee Road
Alexandria, VA 22312

Available electronically at http://www.sti.nasa.gov

Material Characterization and Geometric Segmentation of a Composite Structure Using Microfocus X-Ray Computed Tomography Image-Based Finite Element Modeling

Ali Abdul-Aziz and D.J. Roth
National Aeronautics and Space Administration
Glenn Research Center
Cleveland, Ohio 44135

R. Cotton
Simpleware Ltd.
Exeter, United Kingdom

George F. Studor and Eric Christiansen
National Aeronautics and Space Administration
Johnson Space Center
Houston, Texas 77058

P.C. Young[1]
University of Exeter
Exeter, United Kingdom

Abstract

This study utilizes microfocus x-ray computed tomography (CT) slice sets to model and characterize the damage locations and sizes in thermal protection system materials that underwent impact testing. ScanIP/FE software is used to visualize and process the slice sets, followed by mesh generation on the segmented volumetric rendering. Then, the local stress fields around several of the damaged regions are calculated for realistic mission profiles that subject the sample to extreme temperature and other severe environmental conditions. The resulting stress fields are used to quantify damage severity and make an assessment as to whether damage that did not penetrate to the base material can still result in catastrophic failure of the structure. It is expected that this study will demonstrate that finite element modeling based on an accurate three-dimensional rendered model from a series of CT slices is an essential tool to quantify the internal macroscopic defects and damage of a complex system made out of thermal protection material. Results obtained showing details of segmented images; three-dimensional volume-rendered models, finite element meshes generated, and the resulting thermomechanical stress state due to impact loading for the material are presented and discussed. Further, this study is conducted to exhibit certain high-caliber capabilities that the nondestructive evaluation (NDE) group at NASA Glenn Research Center can offer to assist in assessing the structural durability of such highly specialized materials so improvements in their performance and capacities to handle harsh operating conditions can be made.

Introduction

New techniques for generating robust and accurate geometry meshes based on three-dimensional imaging data have recently been developed, which make the prediction of macrostructural properties relatively simple (Ref. 1). The construction accuracy is the focal point in these new techniques along with

[1]Associate Professor, School of Engineering and Computer Science, University of Exeter, Harrison Building, North Park Road, Exeter, EX4 4QF, UK, telephone: +44(0)1392263684, e-mail: philippe.g.young@exeter.ac.uk

the geometric precision, which is highly dependent on the image quality. Algorithms are continuously being developed and are used to preserve topology and volume, which in turn facilitate multipart geometric modeling. In addition to geometric modeling, different constituent's materials as separate mesh domains can also be identified, and their properties can be assigned based on signal strength in the parent image. This will provide a means for modeling continuous variations in properties for an inhomogeneous medium. Further, these newer techniques have been embedded into many software codes (e.g., Ref. 2) and are being used and applied to analyze various material types including composites.

Additionally, continuous advancements in the field of x-ray computed tomography (CT) have made it possible to be used in many other applications besides the medical field. It has made a speedy move into the material research area and has become a crucial inspection tool, allowing the measurement of volumetric information such as geometric dimensions, voids, and inclusions of complex materials in addition to providing pictorial views of the internal and external structure of materials (Ref. 1). One of the key features of CT scanning is the ability to use its two-dimensional cross-sectional images to generate an accurate three-dimensional visualization and quantification of the internal structure of materials (Refs. 1 and 2). However, most material CT studies stop after the three-dimensional volumetric rendering of the internal structure of the sample. Few material researchers have used CT beyond simple image analysis and quantitative image assessment. A few studies extended the use of CT to the generation of high-fidelity finite element models from CT slice data to calculate the localized stress and strain field of the actual material morphology (Refs. 3 to 9).

Thus, the core of this study is focused on the use of x-ray CT for creating engineering models and subsequent simulations using these models to assess durability for a NASA thermal protection system (TPS) (Fig. 1). This TPS configuration is under consideration for use in NASA's multipurpose Orion crew module (CM). The TPS utilizes alumina enhanced thermal barrier 128 kg/m³ (8 lb/ft^3) (AETB–8) tiles bonded to the CM backshell, which acts as the substrate for the TPS. The substrate is a honeycomb panel with a titanium or aluminum honeycomb core bonded to either carbon composite face sheets or titanium face sheets. The TPS protects the vehicle and crew from external temperatures during reentry as well as impacts from micrometeoroids and orbital debris. The threat of hypervelocity impact from micrometeorites, and especially manmade space debris, is an increasing concern for spacecraft. Therefore, it is critical to understand how well the TPS can withstand hypervelocity impacts and how well it can protect the underlying structure from damage. Microcomputed tomography (micro-CT) image-based finite element modeling is used to appraise the structural performance of this material subject to a high-velocity-impact loading.

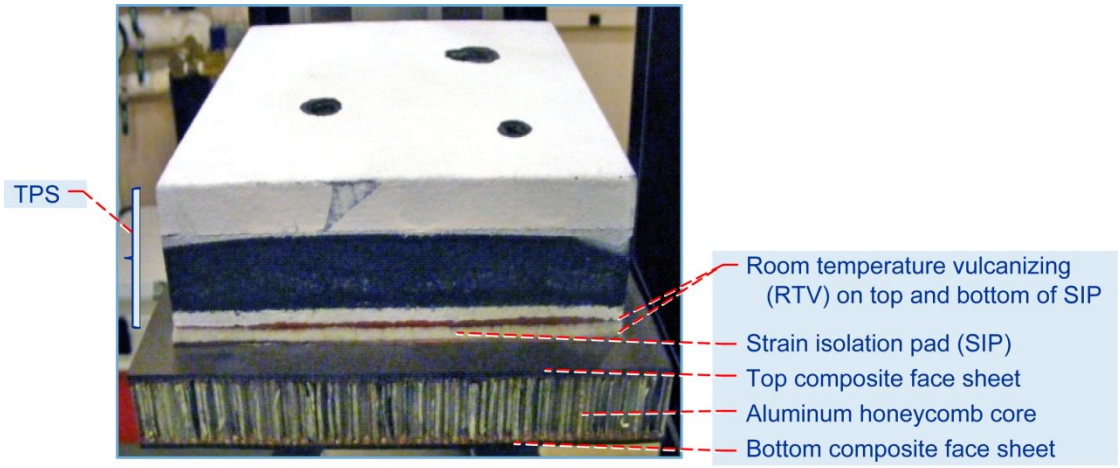

Figure 1.—Impacted thermal protection system (TPS), showing various materials layout.

A detailed representation showing the material layout of the TPS is shown in Figure 1. The top portion including the white coating is the actual proprietary TPS material with a thickness of about 30 mm including a strain isolation pad (SIP). The SIP is covered from the top and bottom with a room-temperature vulcanizing (RTV) silicon adhesive and is used as the interfacing layer between the TPS and vehicle structure. Note Figure 1 for more details (Refs. 10 and 11).

Different software programs are used to perform various image segmentation and processing operations, volume rendering (Ref. 2), and analytical modeling (Ref. 12). This study shows a fusion of technologies performed by the NASA Glenn NDE group that is capable of performing and utilizing high-resolution x-ray CT data ultimately geared towards engineering studies.

Image Processing and Analytical Approach

The steps and details of the image processing, segmentation, three-dimensional volume rendering, and mesh generation of the scanned impacted TPS material specimen are illustrated in this section. Finite element analyses and the corresponding results are also outlined. Figure 2 shows a side and a top view of selected CT slices of the impact-damaged sample. The damaged sample was x-ray CT scanned using a Fein-focus FXE 200 keV x-ray source (Fig. 3), and 160 image slices were produced. Each slice was converted from raw binary to TIFF format (1200 by 700 pixel resolution). The in-plane resolution of the scanner was 0.2 mm (in both x- and y-directions), whereas the separation between each slice was about 0.0376 mm. The voxel dimension on this scan set should be the same (200 μm) in all three directions. In-house image-processing software (Ref. 1) was used to convert the CT slices into TIFF format to allow compatibility with ScanIP/+FE software (Ref. 5).

Data Preparation and Cropping

The images in the two-dimensional set were cropped to remove space not occupied by the sample. This resulted in a smaller volume that is close to the actual sample size.

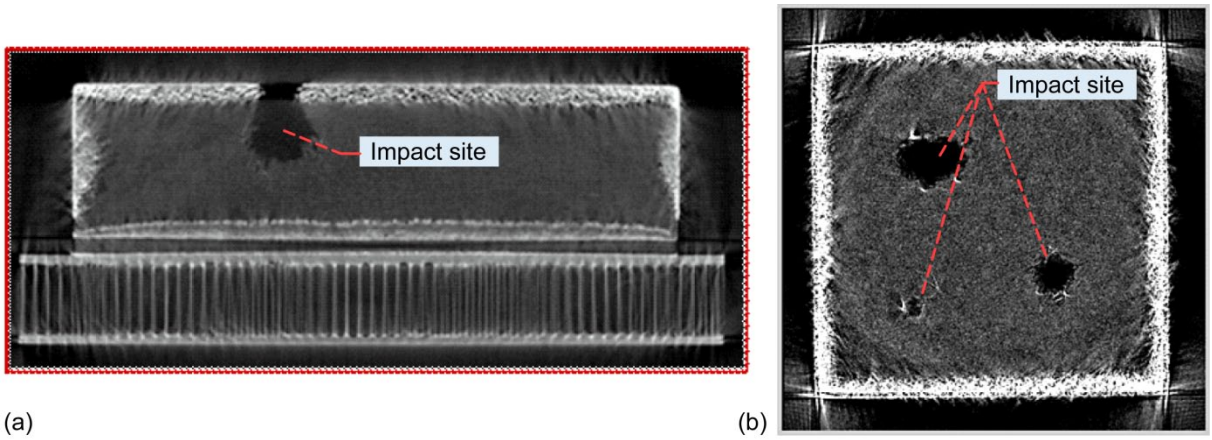

Figure 2.—X-ray computed tomography (CT) image of impact-damaged TPS material. (a) Side view. (b) Top view.

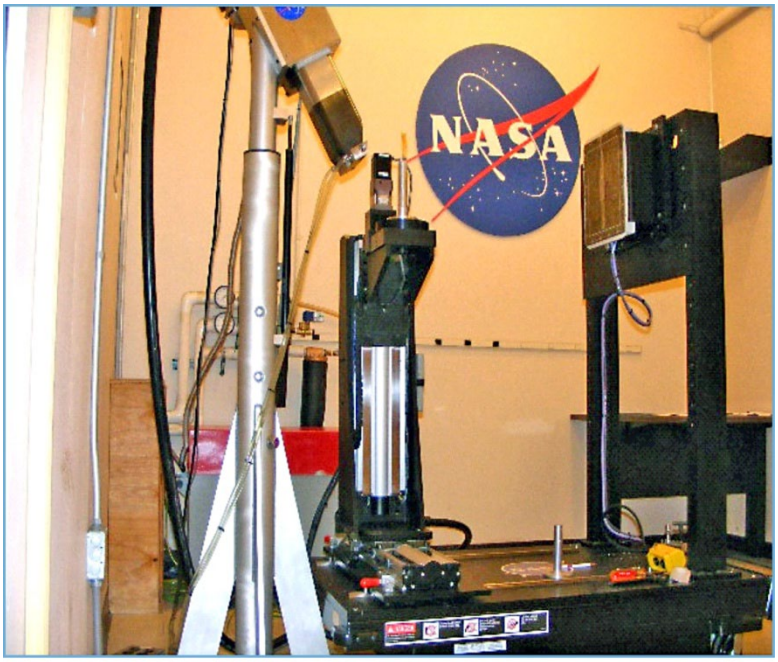

Figure 3.—CT scan system at NASA Glenn Research Center.

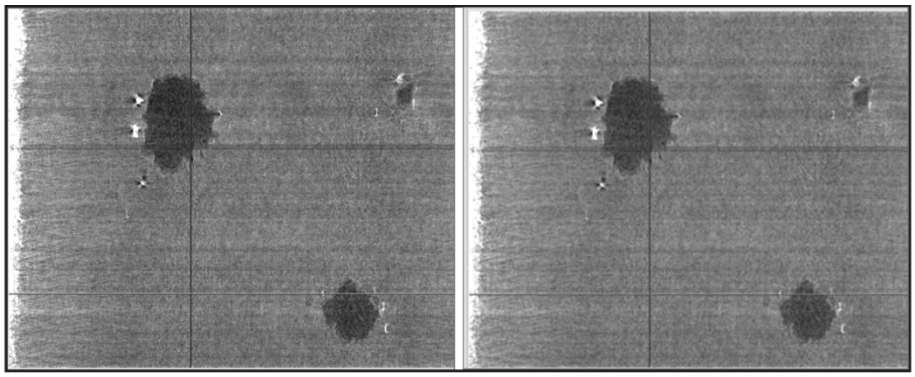

(a) (b)

Figure 4.—X-ray CT of impact-damaged Orion crew exploration vehicle TPS material. (a) Prefiltered CT slice. (b) CT slice filtered with median filter.

Filtering

Various filtration options are available within the ScanIP software; however, the choice of which filter should be applied over others is highly dependent on the nature of the problem, materials, and image quality associated with the CT scan. Because of the noisy nature of the image, some filtering was necessary. The curvature anisotropic diffusion filter was therefore selected to be used. Note that it is considered as a noise reduction filter rather than a smoothing filter because its purpose is to reduce noise while preserving features, which is not the case of smoothing filters such as a Gaussian filter. Smoothing filters, in contrast to noise filters, will get rid of noise and also smooth or attenuate contours. The curvature anisotropic diffusion filter was applied here with a conductance of 5, a time step of 0.0625, and 10 iterations (see users' manual in Ref. 2).

Figures 4(a) and (b) display a sample CT slice showing prefiltering and postfiltering views. The figure simply illustrates the image enhancement due to filtering which helped smoothing.

Image Segmentation

Segmentation is the process of identifying, within an image, what pixels belong to each object of interest. In this study, several finite element models were considered, differing by mesh density, geometrical definition, or by the way material properties are defined. The segmentation process itself only influences the geometrical definition of each model, and there are actually four models that are geometrically different. These meshes correspond to individual models of each of the three impact craters and a model of the whole sample. An example of the mesh of the full sample with the three impact craters can be seen in Figure 5. Figure 5(a) shows a volume rendering of the CT image set, and Figure 5(b) shows the resulting finite element mesh with transparency visualization. Due to the artifacts in the data caused by changes in density of the material, the segmentation process required several steps. The artifacts meant that the grayscale values of the matrix varied throughout the three-dimensional volume model.

Therefore a global threshold would not be suitable; local thresholding on individual or a selection of slices was required to ensure the correct geometry of the impact craters was captured. After the local thresholding, the paint tool was used to manually enhance and straighten the segmentation. For example, regions where the boundary between crater and material was distorted from artifacts were all cleared out via the paint and segmentation option available within the software. The process was rather cumbersome, but it did result in capturing the fine details that represented the core of the materials' structural characteristics. As described, four different masks each representing separate regions were created, with the A being the whole matrix and B, C, and C* being the masks representing the individual three craters, respectively. Figures 6(a) and (b), respectively, show a sector of the segmented material and a corresponding transparent view of one of the craters represented by a mask, where features such as the honeycomb core, the composite, and the TPS + SIP materials are clearly identified.

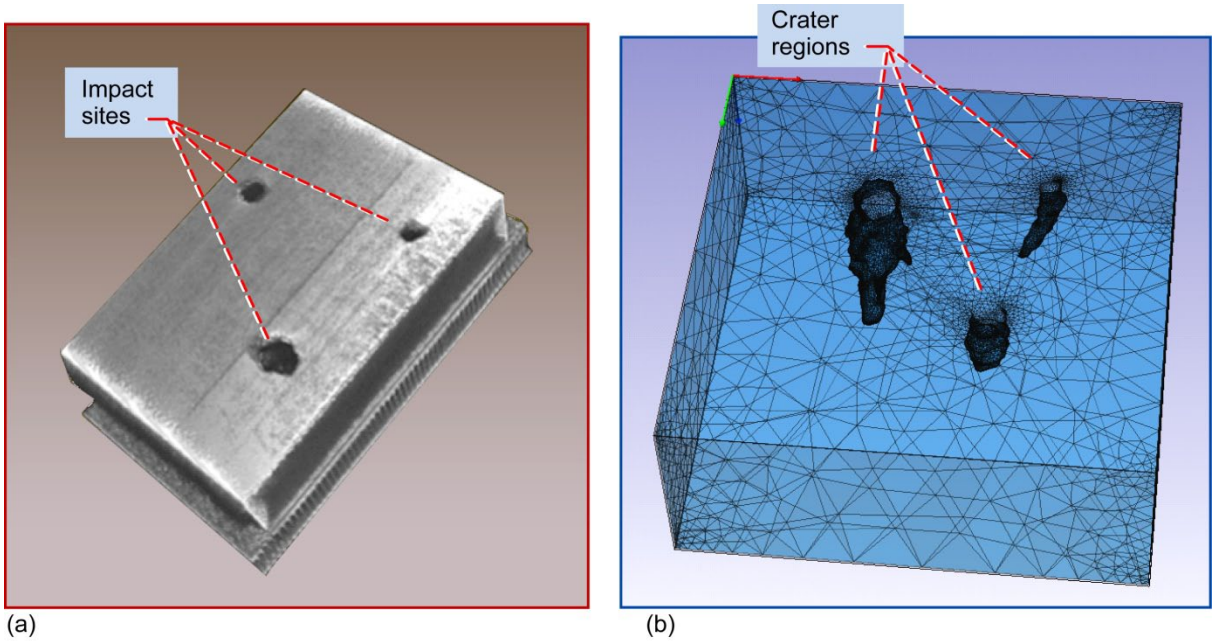

Figure 5.—Three-dimensional volume of impacted TPS. (a) Rendered x-ray CT model. (b) Generated finite element model.

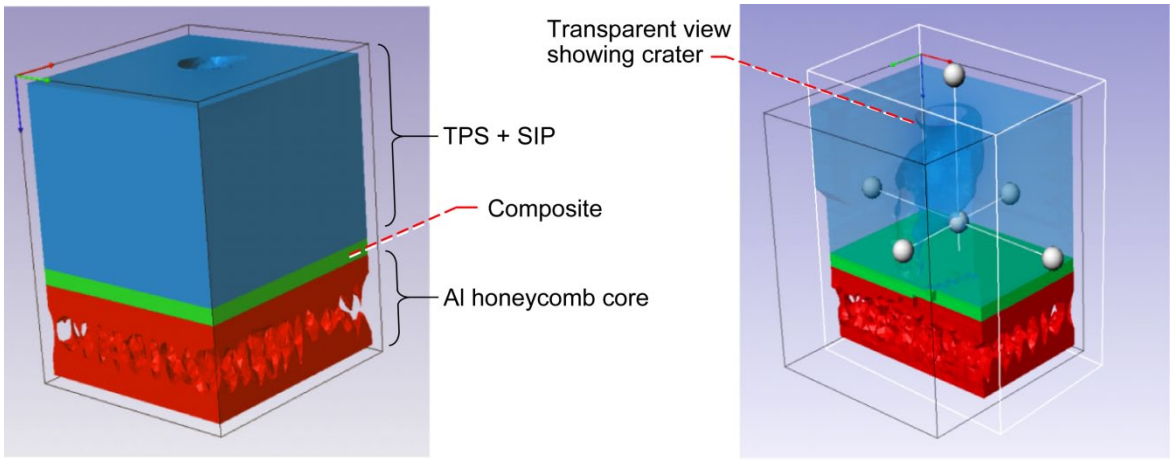

Figure 6.—Sector of vehicle structure segmented into three materials. (a) X-ray CT three-dimensional rendered volume including impact crater. (b) Transparent view showing crater within TPS material.

Impact Craters Segmentation

The following sequence was applied to segment the crater regions:

A: Pixels of values ranging from 121 to 255 were thresholded to create a part representing the matrix.

B: Pixels of values ranging from 121 to 255 were thresholded to create a part representing the matrix, and then the holes were floodfilled, with the result of the floodfill being added to the mask. The resulting masks consist of a block incorporating both the matrix and the holes.

C: Pixels of values ranging from 121 to 255 were thresholded to create a part representing the matrix. Then the holes were floodfilled, a feature within the Simpleware software to help optimize the model and invoke a uniform connectivity of surfaces throughout the entire model to generate a second part consisting of the holes only (0 to 120).

C*: Same as C, but using different threshold values to define the matrix (125 to 255) and the holes (0 to 124). The grayscale values varied from slice to slice because of the change in contrast from the artifacts. Also, the 0 to 255 range is not the original values from the scanner. ScanIP works in 8-bit grayscale so the higher bit depth data from the scanner is converted to 256 values using a windowing-level technique.

Mesh Generation

The ScanFE module (Ref. 2) was further used to generate a number of finite element meshes based on the three-dimensional segmented image data. The mesh density generated in ScanFE is closely connected to image resolution to explore convergence of results (field parameters of interest); the image was downsampled to create several volumes, with each representing a sector of interest to generate high- and low-resolution models. As a result, an interesting point can be made here about image-based models versus computer-aided design (CAD) models. In CAD models the geometry of the model is assumed to be exact, and mesh density is increased principally to obtain a better model of the field parameters of interest (i.e., the stress field within a loaded structure). In image-based models, however, both the response and the geometry of the system are approximated.

By generating models based on increasing image resolutions, one not only improves the modeling of the response, but also the representation of the geometry (one effectively converges to the geometry). Hence, one can perform essentially a dual, or coupled, convergence study; however, this type of study provides powerful arguments for the validity of the simulations because convergence of results demonstrates not only that the mesh is of sufficient density to capture the field parameter of interest, but also—and as importantly—that the image resolution on which the model is based is high enough to capture relevant features in the scanned object.

Four models were generated within ScanFE using 40 iterations of Simlpeware's proprietary multipart anti-aliasing (aa) algorithm, followed by two iterations of Laplacian smoothing. The implemented aa techniques ensure high accuracy of reconstruction, unlike many smoothing schemes. They preserve volume, topology, and geometry while ensuring the generation of models whose geometric accuracy is contingent only on image quality (i.e., on the accuracy of the segmentation). Mesh optimization parameters ensured that the element quality index reached a value of 0.15, allowing off-surface nodes (within a 10 percent pixel distance).

Figure 7 shows a view of the finite element mesh generated by the ScanFE-Free mesh option. The modeling is invoked such that a finer grid is generated around the damaged sites and a coarser mesh further out. The meshing technique applied takes the initial image-based resolution of the mesh and then automatically adapts the mesh around areas of curvature (i.e., craters) and then grows the elements where fewer features exist (i.e., the flat boundaries of the part). This will allow more accurate analyses and a higher degree of accuracy in capturing stress risers near geometric discontinuities, and it will also help reduce the size of the model and the computation time. Figure 8 shows a denser version of the three-dimensional rendered volume and the reciprocate finite element model. A notable feature in this version is that the modeling is extended to include a see-through crater as opposed to the earlier model shown in Figure 8. This reveals the extent of the damage caused by the impact and how far down the TPS stack damage was observed.

Additionally, this model is generated to highlight the capabilities and the ability to enable generating such highly complex geometries with good accuracy. The size of the model is relatively large and has 1 891 827 tetrahedral elements and 341 979 nodes. Much larger computational time and core memory must be allocated to conduct the analyses using this model compared to the reduced version shown in Figure 7.

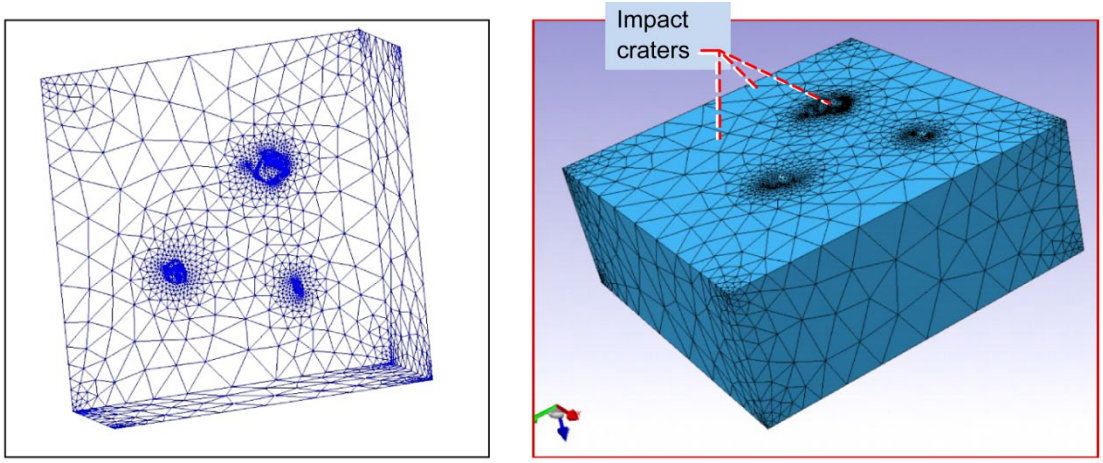

Figure 7.—Finite element mesh of outer impact layer of TPS generated by ScanIP/FE.

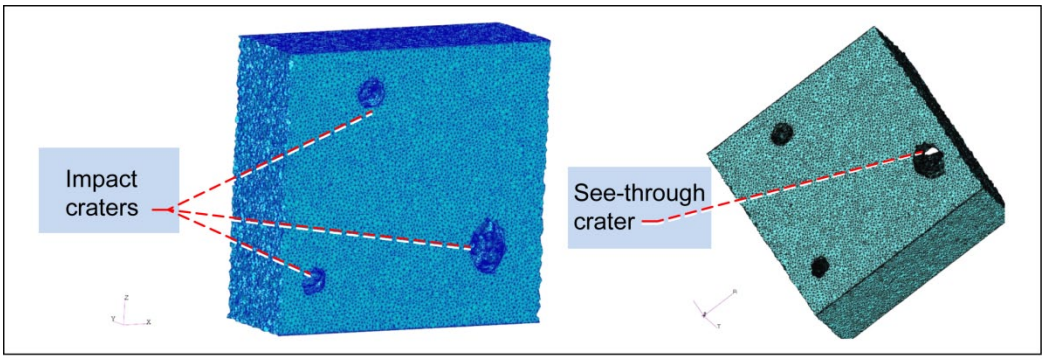

Figure 8.—Higher order and finer mesh model of outer impact layer of TPS with 1 891 827 tetrahedral elements and 341 979 nodes.

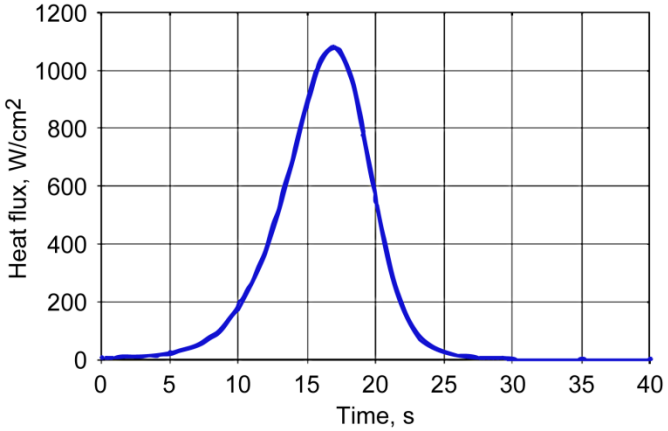

Figure 9.—Heat flux versus time for Reusable Launch Vehicle (RLV) entering Earth's atmosphere at 11.5 km/s (Ref. 13).

Finite Element Modeling and Analyses

The model shown in Figure 7 consists of 31 928 nodes and 485 688 linear tetrahedral 4-node elements. The model represents a reduced version of the specimen shown in Figure 5(a). It mainly covers the impact region (top layer) and the surrounding area. The honeycombs, along with other layers below the impact region shown in the specimen photo (Fig. 1), are omitted in the analyses for simplicity purposes and to reduce the size of the model. Coupled thermomechanical analyses are conducted under combined thermal and mechanical loads. The thermal load is due to the heat generation and the mechanical load is due to the maximum attained pressure exerted on the system during reentry of the vehicle into Earth's atmosphere.

The analyses covered only the condition in which the heat flux is the highest. This is to cover operational impact under the worst-case episode and at the level where the TPS is subjected to the highest thermal load possible. Figure 9 offers a representation of the heat flux experienced by the vehicle upon reentry (Ref. 13). The mechanical load due to the pressure exerted by the vehicle's high speed is simulated by applying a 21 550-Pa uniform pressure load along the hot face.

The TPS specimen finite element model was contained to simulate a secure attachment to the vehicle. Mechanical constraints were implemented such that the nodes on the bottom or inner surface were restrained from movement in the z-direction, and on the opposite face prescribed pressure loading boundary conditions were applied normal in the inward direction. Thermal loading was realized by assigning a temperature value of 21 °C to the bottom face of the specimen, depicting room-temperature

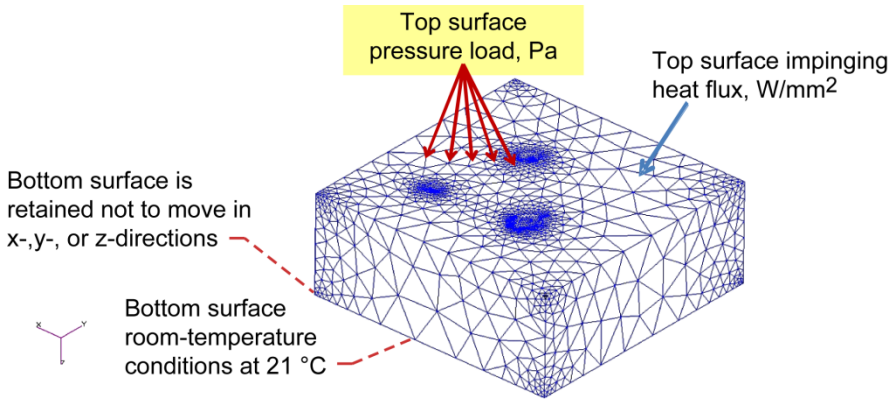

Figure 10.—TPS finite element model showing applied boundary conditions and related mechanical constraints.

TABLE I.—TPS MATERIAL (LI–900) PHYSICAL PROPERTIES (REF. 12)

Material	Density, kg/m^3	Tensile strength, kPa	Compression strength, kPa	Coefficient of thermal expansion,[a] cm/cm-°C	Thermal conductivity,[b] W/cm-°C
LI–900	141	Through-thickness, 186 In-plane, 469	Through-thickness, 310 In-plane, 724	In-plane, 5.76×10^{-7}	0.0011394

[a]21 to 815 °C.
[b]at 1 atm and 537.37 °C.

conditions. The thermal load at the top surface was simulated by applying an impingement heat flux. The material properties of the TPS, LI–900 (Ref. 11), used in the analysis are shown in Table I. The LI–900 is not the material that represents the current system being discussed in this paper; however, it was selected because of its similarity to the actual TPS. Figure 10 illustrates the applied boundary conditions. The calculations were performed using the general-purpose MARC finite element code (Ref. 12).

Results and Discussion

The finite element analysis results are shown in Figures 11 and 12. Figure 11 represents the thermal profile obtained as a result of the orbit reentry impact. As expected, a uniform temperature state dominated the top surface exposed to the atmosphere and a through-thickness gradient is noted as the thermal profile travels through the material. A maximum temperature of 1500 °C is seen at the top surface, and the inner surface maintains a room temperature value of about 21 °C as projected. Additional details concerning the thermal profile variations through the thickness of the LI–900 material are clearly obvious at the crater regions.

The stress state generated as a result of the thermal environment experienced during reentry is shown in the contour plots represented by Figure 12. Clearly, the crater regions experienced high stress riser variations as expected (Fig. 12(a)). This is due to the thermal gradient inflicted by the thermal load applied, the pressure load, and the material properties disparity with temperature (Fig. 11). However, it must be noted that the stress magnitude calculated in these analyses does not reflect the actual magnitude that the vehicle would experience during the real episode of reentry; the purpose of these analyses is to demonstrate and to verify an analytical methodology only. For a more precise estimation, additional implementations of factors pertaining to other materials included in the TPS, the complete data of the thermal and mechanical environment, and the entire system material properties must all be accounted for in the analyses.

Figure 12(b) shows a more detailed view of the modeled TPS and additional facts of the stress gradient at the craters sections. This confirms the fact that these impact sites could be the trigger points

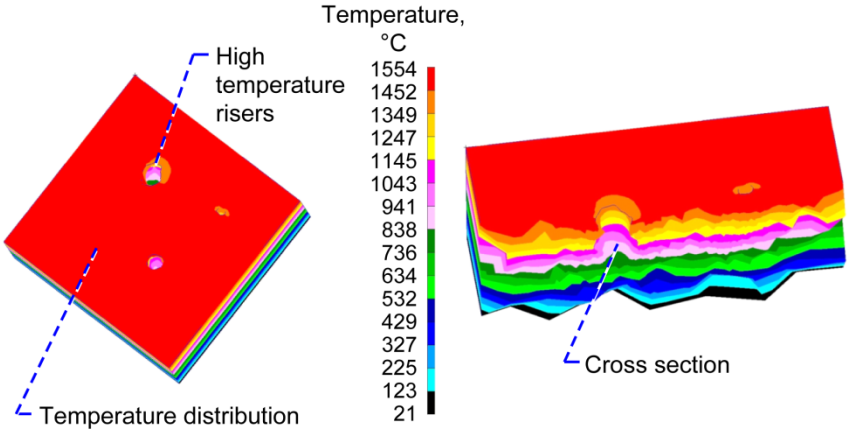

Figure 11.—TPS temperature profile. Coupled thermal and structural finite element analysis results.

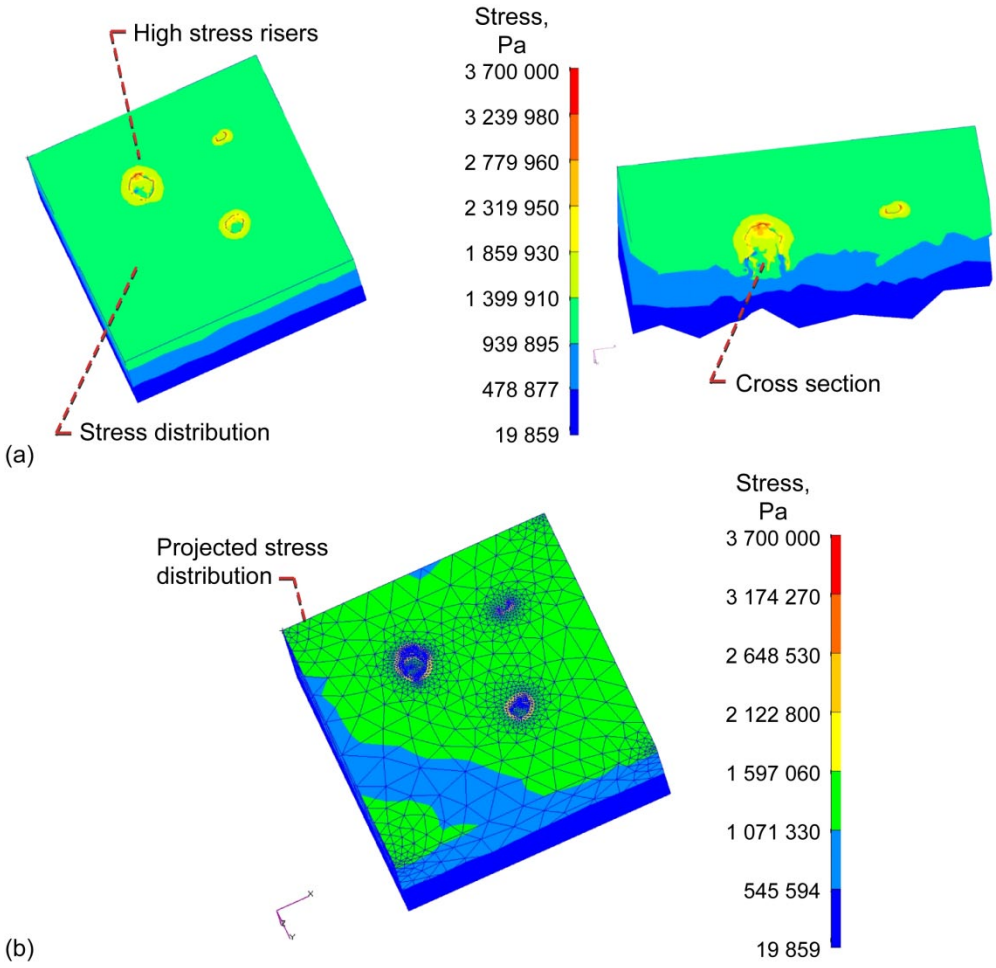

Figure 12.—TPS stress profile. Coupled thermal and structural finite element analysis results. (a) Section view. (b) Full model.

for potential hazards, which would jeopardize the safety of the vehicle during reentry. In particular, the see-through location is the most crucial situation since it would permit the exposure of the internal body of the vehicle to a dangerous and high level of heat generated during the reentry period. Such condition is a cause for a catastrophic event that would lead to the total destruction of the vehicle.

Conclusions

This combined microfocus x-ray computed tomography (micro-CT), followed by image segmentation and processing, with subsequent three-dimensional volume rendering and finite element analysis has shown that combining nondestructive evaluation (NDE) and finite element methodology is an effective tool to characterize and perform complicated NDE-related computations. It further illustrates an in-depth methodology to appraise structural durability issues typically experienced in a damaged thermal protection system (TPS) material so improvements in the TPS performance and its capacity to handle harsh environments can be made. The CT scanning is utilized as the NDE method to construct a high-fidelity three-dimensional finite element model of a complex TPS specimen. The latest advances in software technology were instrumental in assisting to build an accurate three-dimensional model with ease and with relatively little effort from the user. The finite element mesh size was large, but the section model was adequate to represent the damaged TPS. The results showed that the crater regions experience high stress risers as anticipated. Clearly, the crater regions' high stresses were due to the thermal gradient inflicted by the heat generated and the pressure loads attained during vehicle reentry into Earth's atmosphere. Additionally, it should be noted that the stress magnitude reported in this study constitutes no real estimation of the actual stresses experienced during reentry by the vehicle. A more detailed study is needed to accurately estimate such data.

References

1. Roth, Don J.: NDE Wave and Image Processor Software (NDEWIP). Vol 3, June 2010.
2. ScanFE. Simpleware Ltd., Innovation Centre, University of Exeter, London.
3. Abdul-Aziz, Ali; Baaklini, George; and Bhatt, Ramakrishna: Nondestructive Evaluation of Ceramic Matrix Composites Coupled With Finite Element Analyses. SPIE Proceedings Series, vol. 4704, 2002, pp. 32–39.
4. Griffin, A.; Knox, C.; and McMillin, S.: Practical Examples: Using Scan Data for Reverse Engineering. AUTOFACT '97, Society of Manufacturing Engineers, PE98–122, 1997.
5. ScanIP/+FE. Simpleware Ltd., Innovation Centre, University of Exeter, London.
6. Boomsma, K.; and Poulikakos, D.: The Effects of Compression and Pore Size Variations on the Liquid Flow Characteristics in Metal Foams. Trans. ASME J. Fluid Eng., vol. 124, 2001, pp. 263–272.
7. Gibson L.J.; and Ashby M.F.: Cellular Solids: Structure and Properties. Cambridge University Press, Cambridge, UK, 1997.
8. Ashby, M.F., et al.: Metal Foams: A Design Guide, Butterworth-Heinemann, Boston, MA, 2000.
9. Banhart, J.: Manufacture, Characterization and Application of Cellular Metals and Metal Foams. Prog. Mater. Sci., vol. 46, 2001, pp. 559–632.
10. Yuen, Walter W.; Takara, Ezra; and Cunnington, George: Combined Conductive/Radiative Heat Transfer in High Porosity Fibrous Insulation Materials: Theory and Experiment**.** The 6th ASME–JSME Thermal Engineering Joint Conference, TED–AJ03–126, 2003.
11. Laub, B.; and Venkatapathy, E.: Thermal Protection System Technology and Facility Needs for Demanding Future Planetary Missions. Presented at the International Workshop on Planetary Probe Atmospheric Entry and Descent**,** Trajectory Analysis and Science, Lisbon, Portugal, 2003.
12. MSC/MARC Finite Element Code. The MacNeal-Schwendler Corporation, Costa Mesa, CA, 2010.
13. Arnold, J.O., et al: Nanostructured Thermal Protection Systems for Space Exploration Missions. Second International Probe Workshop, NASA Ames Research Center, Moffett Field, CA, 2004.

REPORT DOCUMENTATION PAGE	Form Approved OMB No. 0704-0188

1. REPORT DATE *(DD-MM-YYYY)*	2. REPORT TYPE	3. DATES COVERED *(From - To)*
01-07-2011	Technical Memorandum	

4. TITLE AND SUBTITLE
Material Characterization and Geometric Segmentation of a Composite Structure Using Microfocus X-Ray Computed Tomography Image-Based Finite Element Modeling

5a. CONTRACT NUMBER

5b. GRANT NUMBER

5c. PROGRAM ELEMENT NUMBER

6. AUTHOR(S)
Abdul-Aziz, Ali; Roth, D., J.; Cotton, R.; Studor, George, F.; Christiansen, Eric; Young, P., C.

5d. PROJECT NUMBER

5e. TASK NUMBER

5f. WORK UNIT NUMBER
WBS 724297.40.44.03.06

7. PERFORMING ORGANIZATION NAME(S) AND ADDRESS(ES)
National Aeronautics and Space Administration
John H. Glenn Research Center at Lewis Field
Cleveland, Ohio 44135-3191

8. PERFORMING ORGANIZATION REPORT NUMBER
E-17680

9. SPONSORING/MONITORING AGENCY NAME(S) AND ADDRESS(ES)
National Aeronautics and Space Administration
Washington, DC 20546-0001

10. SPONSORING/MONITOR'S ACRONYM(S)
NASA

11. SPONSORING/MONITORING REPORT NUMBER
NASA/TM-2011-217015

12. DISTRIBUTION/AVAILABILITY STATEMENT
Unclassified-Unlimited
Subject Categories: 16 and 01
Available electronically at http://www.sti.nasa.gov
This publication is available from the NASA Center for AeroSpace Information, 443-757-5802

13. SUPPLEMENTARY NOTES

14. ABSTRACT
This study utilizes microfocus x-ray computed tomography (CT) slice sets to model and characterize the damage locations and sizes in thermal protection system materials that underwent impact testing. ScanIP/FE software is used to visualize and process the slice sets, followed by mesh generation on the segmented volumetric rendering. Then, the local stress fields around several of the damaged regions are calculated for realistic mission profiles that subject the sample to extreme temperature and other severe environmental conditions. The resulting stress fields are used to quantify damage severity and make an assessment as to whether damage that did not penetrate to the base material can still result in catastrophic failure of the structure. It is expected that this study will demonstrate that finite element modeling based on an accurate three-dimensional rendered model from a series of CT slices is an essential tool to quantify the internal macroscopic defects and damage of a complex system made out of thermal protection material. Results obtained showing details of segmented images; three-dimensional volume-rendered models, finite element meshes generated, and the resulting thermomechanical stress state due to impact loading for the material are presented and discussed. Further, this study is conducted to exhibit certain high-caliber capabilities that the nondestructive evaluation (NDE) group at NASA Glenn Research Center can offer to assist in assessing the structural durability of such highly specialized materials so improvements in their performance and capacities to handle harsh operating conditions can be made.

15. SUBJECT TERMS
Microfocus x-ray; Nondestructive evaluation; Thermal protection system; Finite element; Computed tomography; Orion; Image processing; Impact craters

16. SECURITY CLASSIFICATION OF:			17. LIMITATION OF ABSTRACT	18. NUMBER OF PAGES	19a. NAME OF RESPONSIBLE PERSON
a. REPORT	b. ABSTRACT	c. THIS PAGE			STI Help Desk (email:help@sti.nasa.gov)
U	U	U	UU	17	19b. TELEPHONE NUMBER *(include area code)* 443-757-5802